

UNIVERSITÀ DEGLI STUDI DI TORINO

DIPARTIMENTO DI CHIMICA

Laurea Triennale in Scienza e Tecnologia dei Materiali

BACHELOR THESIS



Characterization of Silicon detectors
with excellent time resolution

Supervisor:

Prof. Riccardo Bellan

Co-Supervisor:

Dr. Nicolò Cartiglia

Author:

Giulia Gioachin

Academic year 2018/2019

Abstract

High energy physics increasingly requires instruments with improved spatial and time resolution and for this reason there is a continuous research in innovative particle detectors in order to achieve better performances.

This thesis focuses on the development and characterization of Low Gain Avalanche Detectors (LGAD), which represent an evolution of silicon detectors with internal charge multiplication. LGAD technology is at the basis of the development of Ultra-Fast Silicon Detectors (UFSD). They are innovative silicon detectors that use a gain layer in order to achieve charge multiplication, amplifying the signal produced by a particle crossing the detector. Thanks to this innovation, and to the use of thin sensors, UFSD can provide an excellent space and time measurements of the passage of a charged particle.

This thesis presents the work I did during my internship at Laboratory for Innovative Silicon Sensors in Torino. I studied the response of the gain layer, verifying that is essential to achieve an excellent time resolution. Especially, I probed the uniformity of the internal gain among many hundreds of sensors and I measured for the first time the doping uniformity in the gain layer within a wafer and among wafers. In the second part of my activities, I measured the sensors response when they are exposed to a laser beam.

Contents

Chapter 1. Development of Ultra-Fast Silicon Detectors	5
1.1 Semiconductor Features	5
1.2 Silicon Detectors	6
1.3 LGAD and Ultra-Fast Silicon Detectors	7
Chapter 2. Uniformity studies for UFSD	10
2.1 Probe station set-up for C(V) measurements	10
2.1.1 C(V) measurements	11
2.2 The Transient Current Technique set-up	13
Chapter 3. Measurements	15
3.1 C(V) analysis	15
3.1.1 FBK UFSD3	15
3.1.2 HPK Type 3.2	20
3.1.3 HPK Type 3.1	23

	3
3.2 Curves from Transient Current Technique	27
3.2.1 HPK Type 3.1	
27	
3.2.2 HPK Type 3.2	
29	
Conclusion	31
Bibliography	32
Ringraziamenti	

Chapter 1

Development of Ultra-Fast Silicon Detectors

1.1 Semiconductor Features

Silicon, as a semiconductor, is characterized by an energy band structure where there are permitted energy states and forbidden energy region. The lower permitted energy band is called the valence band (VB), while the upper one is the conduction band (CB). The energy difference between the lower energy state in the CB and the highest energy state in the VB is the so called band energy gap (E_g). At $T=0$ K all the states in the valence band are occupied and all the states in the conduction band are empty. Since the value of band gap is 1.12 eV for pure silicon, at room temperature electrons in the VB acquire enough thermal energy to make a transition from the valence into the conduction band, leaving in valence band an empty location called hole (h). A hole represents the lack of an electron in VB, and it is as an electron but with a positive charge.

We could perturb the crystalline lattice inserting some impurities within the material. Silicon can be doped to n-type or p-type: in the first case a pentavalent impurity called donor, like phosphorus, replaces a silicon atom, which has four valence electrons. The fifth electron not shared is donated to the conduction band and so, in n-type silicon, there are more negative carriers than positives. In this case, the electrons are called “majority carriers” and the holes are the “minority carriers”. While in p-type silicon, a trivalent atom as boron (acceptor), substituted a silicon atom. In this case, the fourth and missing covalent bond uses an electron from the valence band to complete the octet. This negative-charge leaves a hole in the VB, resulting in an excess of positive-charged holes (majority carriers) in p-type semiconductor.

When p-type silicon is in contact with n-type silicon, a p-n junction is formed. Since in the p-type region there are more holes than in the n-type one, the positive charges start to move by diffusion towards the side with fewer holes. In the same way, electrons move to p-type region because, there, their concentration is lower. Near the junction the diffusion mechanism produces a region without mobile carriers called depletion layer. There, the remained charges are phosphorus and boron ionized atoms, as shown in Figure 1. Since they lost their mobile charges due to the diffusion, they lost their charge neutrality and, in the junction, rise an intrinsic electric field that opposed to diffusion’s mechanism.

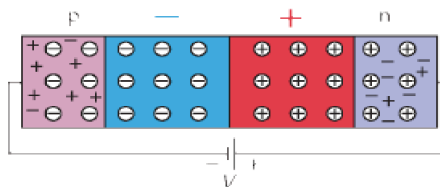
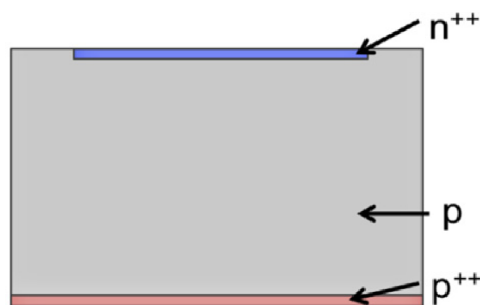


Figure 1. A p-n junction in Reverse Bias condition

When a voltage is provided to a device, it is in bias condition and there are two different conditions. If p-type region is connected to the positive terminal of the power supply and n-type region to the negative one, we are in direct bias condition. In this case, the mobile charges are pushed towards the junction and the depletion layer decreases. Instead, if p-type region is connected to the negative terminal and n-type region to the positive one, we are in reverse bias condition. In this way holes and electrons move away from the junction and the depletion layer increases: this is the relevant configuration for the detection of particles. In these conditions we have completely inhibited the majority carrier's flow, but the flow of the minorities remains creating a small current, called leakage current.

1.2 Silicon Detectors

At the basis of a particle detector there is the interaction of the radiation with an active material. Interactions cause phenomena such as ionization and excitation of atoms. When a charged particle crosses a material, it loses energy and its trajectory changes. When an incident charged particle crosses the sensor, it creates along its path a series of electron-hole pairs (~ 75 electron-hole pairs per micron) that are collected by the electrodes under the influence of an external electric field generated by the bias voltage. During the electrons and holes drift, an electric pulse is created at the electrodes.



Traditional Silicon Diode

Figure 2. n-in-p Silicon detector

In particular, a p-n junction that works in reverse bias condition can be used as particle detector: in the depletion region there are almost no free carriers but the ones that can be produced by the energy loss of an ionizing particle. Thus, a signal generated by the passage of a particle can be detected over the small background produced by the leakage current induced by minority carriers. Usually sensors are junctions where the two regions have different doping (as shown in Figure 2): in the n-in-p design, p-type region is thicker and it is called “bulk”; n-type region is thinner and

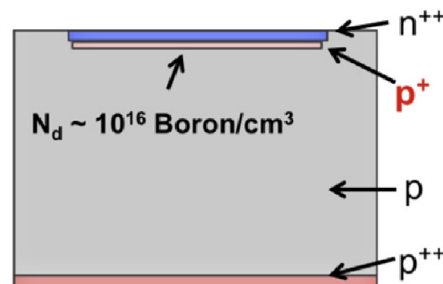
much more doped than the other. Indeed, bulk's doping concentration is $10^{11} - 10^{12} \frac{\text{atoms}}{\text{cm}^2}$, while the doping of the n^{++} electrode is $10^{19} \frac{\text{atoms}}{\text{cm}^2}$. Under the influence of the electric field, electrons and holes drift towards the electrodes, creating an induced current (electric signal) that arises when the charges begin to move. The induced current signal can be calculated using Shockley-Ramo's theorem (Eq. 1):

$$i = qvE_w \quad (1)$$

where the current (i) induced by a charge (q) is proportional to the value of the electric charge, the drift velocity v and the weighting field E_w (field that describes the coupling of the charges to the read-out electrode).

1.3 LGAD and Ultra-Fast Silicon Detectors

The Low Gain Avalanche Diode (LGAD) design [1] represents an evolution of silicon detectors with internal charge multiplication [2]. The charge multiplication is based on the avalanche process initiated by an electron or a hole traversing a region with a strong-enough electric field. The moving charge acquires a kinetic energy greater than E_g and is able to create, by interacting with the crystal reticle, several electron-hole pairs. This is the beginning of the avalanche: iteratively, the newly produced charges are themselves accelerated by the electric field and can create more electron-hole pairs.



Low Gain Avalanche Diode

Figure 3. LGAD design

We can observe the introduction of a thin p^+ layer close the junction

LGAD are n-in-p silicon detector with a modification of the traditional sensors, where an additional doping layer of p^+ material (Boron), called Gain Layer, is introduced close to the junction for create a controlled avalanche, Figure 3. The gain layer, since the p^+ is more doped than the bulk or electrodes, creates a region with a strong electric field that allows charge

multiplication. The charge multiplication allows to obtain a greater signal. Using a specific program Weightfield2 (WF2) [3], it is possible to simulate the energy released by a particle into a silicon detector and its response, as shown in Figure 4.

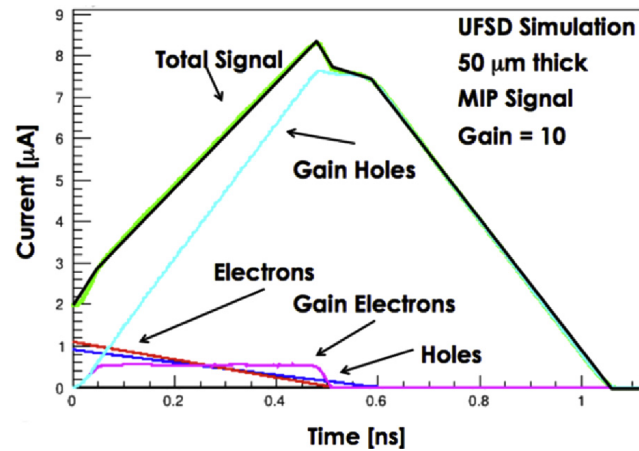


Figure 4. Current signal using WF2

UFSD simulated current signal by a particle (MIP) for a 50 μm thick sensor. Using different color, we can see the components of current brings by charge carriers.

Ultra-Fast Silicon Detectors (UFSD) are sensors based on the charge multiplication mechanism of the LGAD, and they are design explicitly to have an excellent time resolution. For this reason their thickness is only 40-50 micrometers. The main feature of UFSD is the time resolution that is much better than that of traditional silicon detectors. This can be demonstrate using the Ramo's theorem:

$$\frac{dV}{dt} \propto \frac{G}{d}$$

where we see that the signal rise time (dV/dt) depends only upon the gain and the sensor thickness. Therefore, thin detectors with high gain provide an excellent time resolution. However, we must consider a problem: when a MIP (Minimum Ionizing Particle) crosses a device, it releases a quantity of charge proportional to the distance traveled. If the path is short, the signal is small. In order to solve this problem, the UFSD design uses the gain layer to provides a significant increase of the signal amplitude.

Since the gain is very important, it is necessary to have a very good gain uniformity for collecting the same current signal everywhere in a large sensor and for guaranteeing the best time resolution on the whole detector.

Chapter 2

Uniformity studies for UFSD

The study of the gain uniformity on UFSDs requires to measure the doping of the gain layer in many devices. This measurement is obtained by analyzing the value of the capacitance (C) as a function of the bias voltage (V): the value of C , in fact, contains the information on the gain implant. In this chapter I first illustrate the measurements of the $C(V)$ curves using the probe station set-up, and then the study of the signals in UFSD using the Transient Current Technique (TCT) set up.

2.1 Probe station set-up for $C(V)$ measurements

The probe station, Figure 5, is a fundamental instrument that allows us to characterize an UFSD and to study its properties, through the extraction of the $C(V)$, $I(V)$ and $C(f)$ curves.

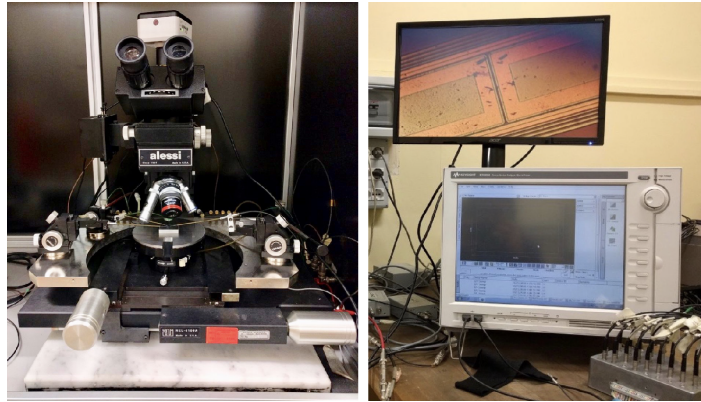


Figure 5. The left panel illustrates the probe station which is connected to the Keysight B1505A Power Device Analyzer and Curve Tracer, which is displayed in the right panel.

This station is composed by:

- an optical microscope with different magnifications;
- a video camera which allows us to visualize the detector on a screen and the position of the needles;
- a support structure, called chuck, connected to a vacuum pump that keeps still the sensor during the characterization;
- two needles for the electrical connections of the sensor.

The needles of the probe station are connected, via long cables, to the parameter analyzer Keysight B1505A. This connection changes depending on the measurement that is needed. The Keysight B1505A is provided with many modules, and it can source and measure voltages, current and capacitance.

2.1.1 C(V) measurements

First, sensor needs to be polarized. A voltage difference is provided through the chuck and a needle, which is connected to the pad electrode. They are connected to the module High Voltage Source Measure Unit (SMU), while the second needle is connected to the module Medium Power SMU. This needle is in contact with a guard ring (rings that stop superficial currents and external electric field) to ground. The capacitance is obtained using another module called Multi Frequency Capacitance Measurement Unit (MFCMU), which provides a sinusoidal signal with a specific amplitude and phase. For each bias step, the capacitance values are obtained from the attenuation of amplitude and from the phase-shift of the test sinusoidal wave.

To acquire the best possible C(V) curve, first it is necessary to perform a C-frequency scan C(f). Infact, the sensor is equivalent to a RC circuit, and behaves like a low-pass filter. For this reason a C(f) necessary to choose the best value of frequency of the test sinusoidal wave: this value is the one corresponding to the plateau of the curve, as shown in Figure 6. Once the best frequency value has been chosen, we set up the apparatus for the C(V) measurements.

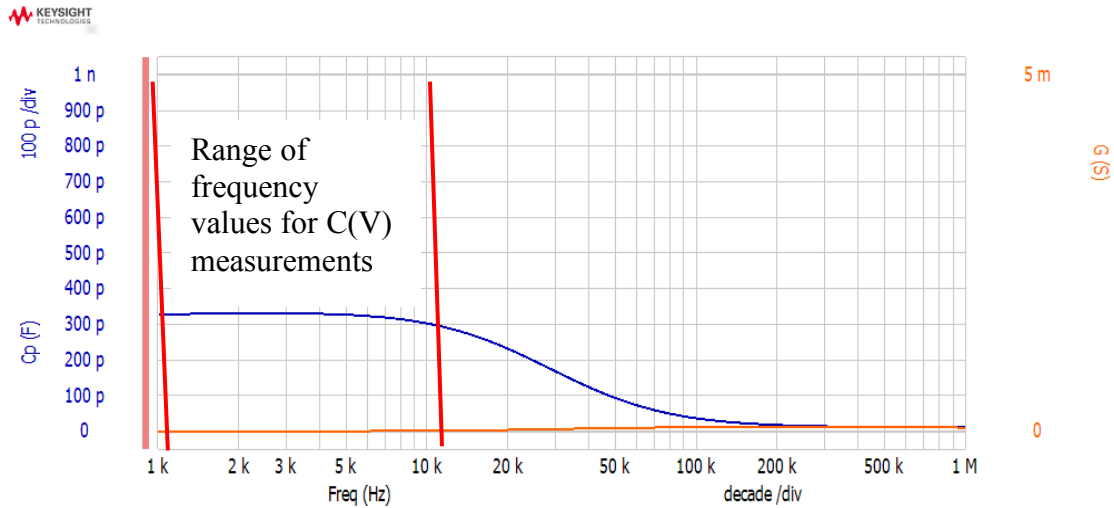


Figure 6. Example of a $C(f)$ curve

We see the plateau of the curve and the best frequency values we can use for the $C(V)$ curve.

A p-n junction of a traditional silicon detector, behaves like a parallel plate capacitor and therefore the junction capacitance (Eq. 2) depends on the dielectric constant, the area of the sensor and the depletion layer width (W):

$$C = \frac{A\epsilon_s}{W}. \quad (2)$$

Using Poisson's equation for studying the p-n junction, we find:

$$C \propto \sqrt{\frac{1}{V}}.$$

Therefore, the capacitance for a silicon detector follows $1/\sqrt{V}$ behavior and then becomes constant once the bulk is depleted, as shown in Figure 7.

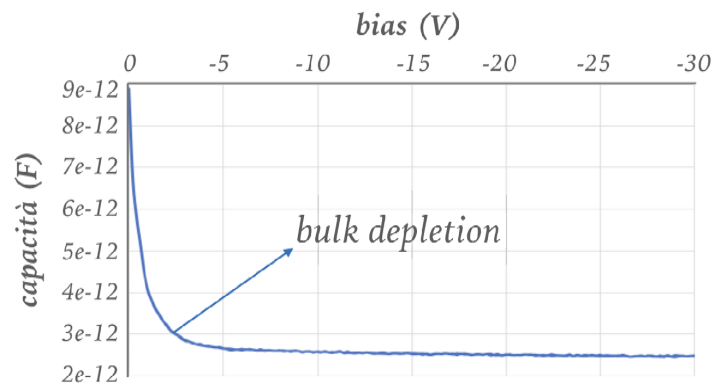


Figure 7. C(V) curve of a silicon detector.

If we consider a LGAD C(V) curve, we can identify two different regions: a first part of the curve related to the depletion of the gain layer and then a second one to the depletion of the bulk, Figure 8.

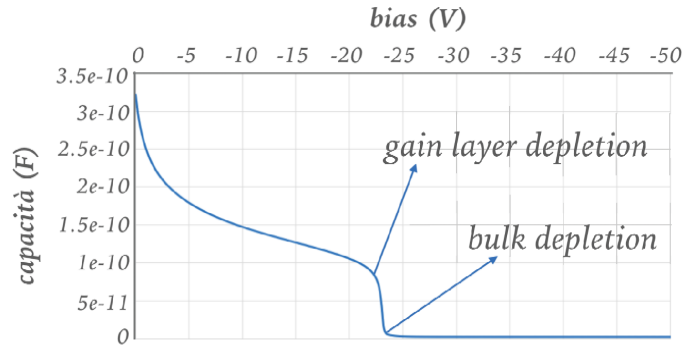


Figure 8. C(V) curve of an LGAD

Because the depletion voltage depends on the doping concentration, a region more doped needs a larger potential difference to reach full depletion. From these curves, it is possible to obtain the doping concentration of the sensor or identify the gain depletion voltage ($V_{GL} = \frac{qN_A w^2}{2\epsilon_{Si}}$ where N_A is the active doping concentration and w is the gain layer thickness) and so to study the uniformity of the gain layer.

2.2 The Transient Current Technique set-up

The Transient Current Technique (TCT), Figure 9, is a technique that allows to study the sensors response when they are exposed to an induced signal by a laser beam. This system is used to characterize the UFSD by simulating a particle that crosses the sensor. In this way, it is possible to measure the collected charge by a detector and study the effect of doping of the gain layer on the total collected charge.

In order to perform the measurement, the sensor is glued on a board and it is polarized using a power supply. Thereafter, the laser is positioned on the sensor with the help of an infrared camera, that allows to watch the laser beam. When the laser crosses the LGAD, it generates the electron-hole pairs in the depleted p-n junction and therefore simulates the passage of a minimum ionizing particle (MIP). The induced signal is amplified by an amplifier that is connected to the detector through the board. The amplifier converts an input current in a voltage signal which is read by an oscilloscope. Then, the oscilloscope is synchronized with a software that allows to save the signal in a data file.

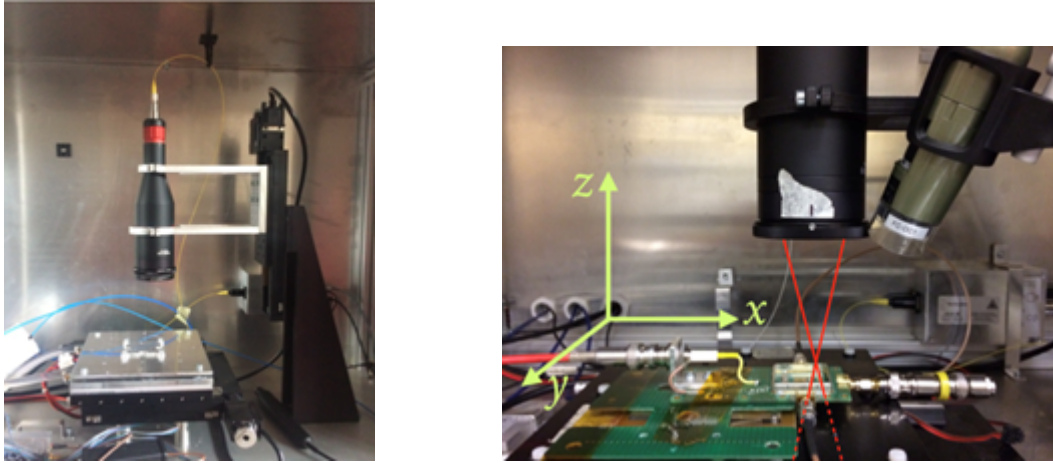


Figure 9. TCT set-up

On the left, there is the laser beam facility and the support for the board; while in the right, it is possible to identify the infrared camera and the board with the glued sensor.

When the laser is positioned on the sensor, the oscilloscope acquires the signal; the area of the signal curve, measured in Weber ($Wb = V*s$), is proportional to the collected charge. The larger the doping of the gain layer, the larger the charge multiplication and therefore the final signal.

Measurements

This chapter is devoted to the analysis of the measurements that I performed on UFSD sensors during my internship in the Laboratory for Innovative Silicon Sensor of the INFN and the department of Physics in Torino. In particular, the studies concern the uniformity of the gain layer within a wafer and among wafers.

3.1 C(V) analysis

This type of analysis allows us to verify the uniformity of the doping in a sensor. If the doping of the gain layer is identical for all the detectors, it is enough to provide the same bias voltage for deplete the junctions, thereby the signal from the charge multiplication is similar among the devices. If a sensor is more doped than the others, a larger voltage must be supplied to deplete it and obtain a measurable signal.

The detectors that I studied are: (i) the *UFSD 3* from Fondazione Bruno Kessler (FBK) production and (ii) Hamamatsu Photonics K.K. (HPK) detectors (Type 3.1 and Type 3.2).

3.1.1 FBK UFSD 3

In a production, the detectors are produced in wafers and in each of them there are different geometry of sensors, depending on the number of pads, for example: single pad, 2x2 or 4x24, as shown in Figure 10.

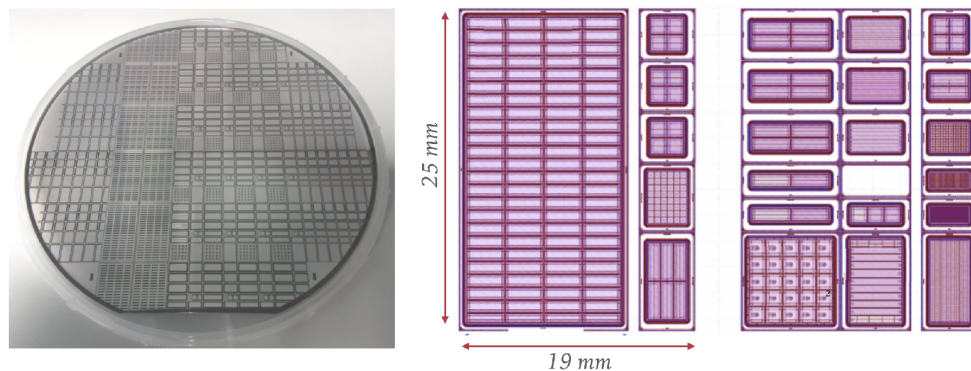


Figure 10. In the left, is represented a wafer; while, in the right, it is possible to identify the different geometries of the sensors.

During my internship, I measured the devices coming from four wafers, in each of them 16 2x2 sensors. Each sensor has 4 different pads. First I verified, measuring all four pads within a sensor, that they have the same doping of the gain layer. Then, for this reason, for all the sensors I extracted

the $C(V)$ curve only from one pad. For each of the wafer I extracted a graph of the $C(V)$ like the one reported in Figure 11. To appreciate the non-uniformity of the gain, it is necessary to zoom in the curves in the voltage range where the gain layer reaches the depletion, this is shown in the bottom part of Figure 11.

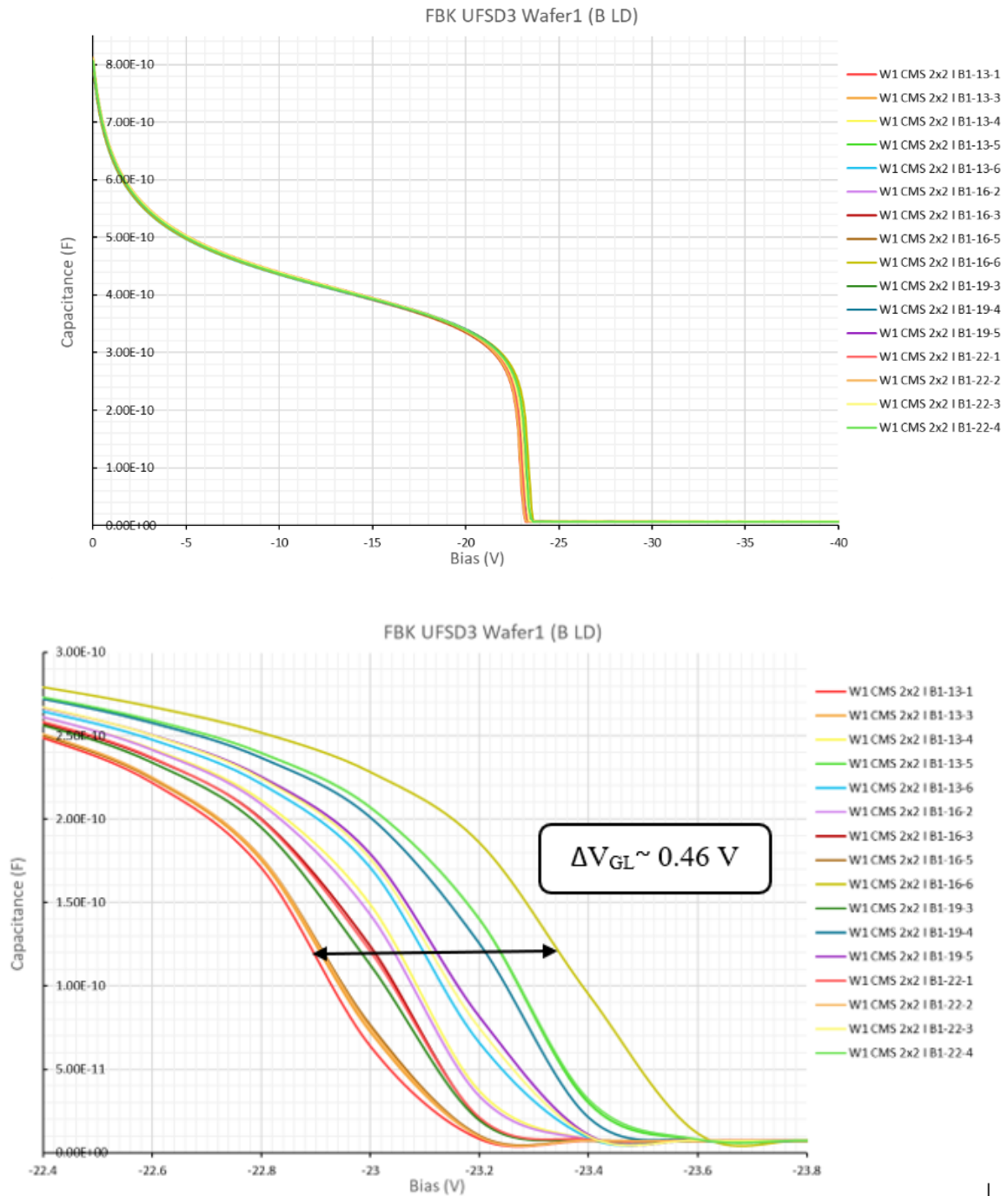
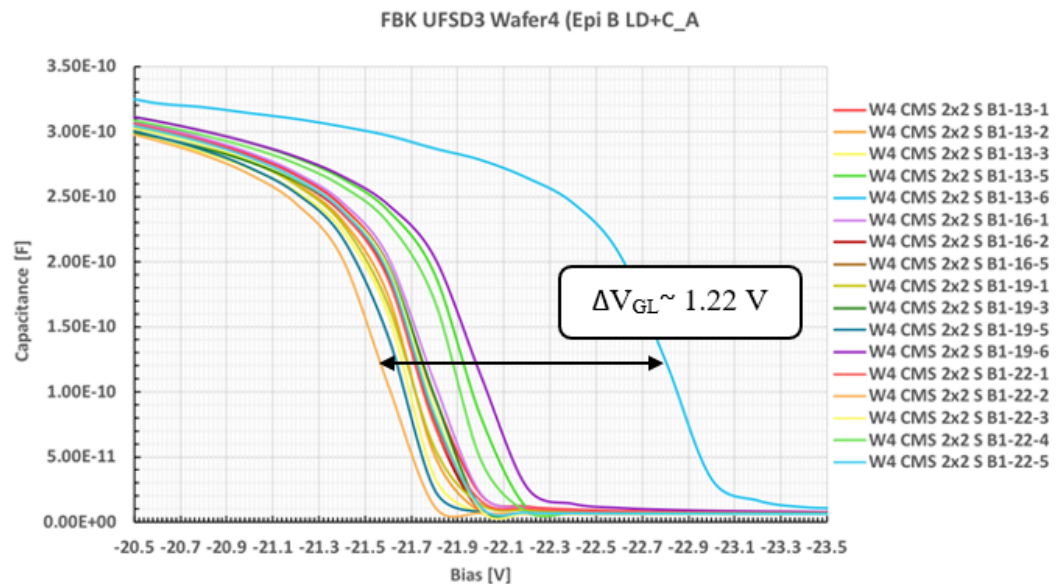


Figure 11. The upper picture reports the C(V) curves of the sensors within a wafer ; the lower picture shows a zoomed region around the voltages where the gain layer gets depleted. The spread of the curves give a measurement of the non-uniformity of the doping of the gain layer.

We can see that the sensors of the wafer 1 deplete the gain layer at different voltages. There is a different of 0.46 V that denotes a value of 2% ($\frac{\Delta V_{GL}}{V_{GL}} * 100$) non uniformity of the doping.

Similar curves are obtained for the other wafer. For two of them, the difference in the gain depletion voltage is greater, as shown in the Figure 12 (top). Observing the position of the sensors in the wafer, it is possible to say that the sensors in the green zone of the wafer (peripheric zone on top of the wafer) reach the depletion at a larger voltage (Figure 12, bottom).



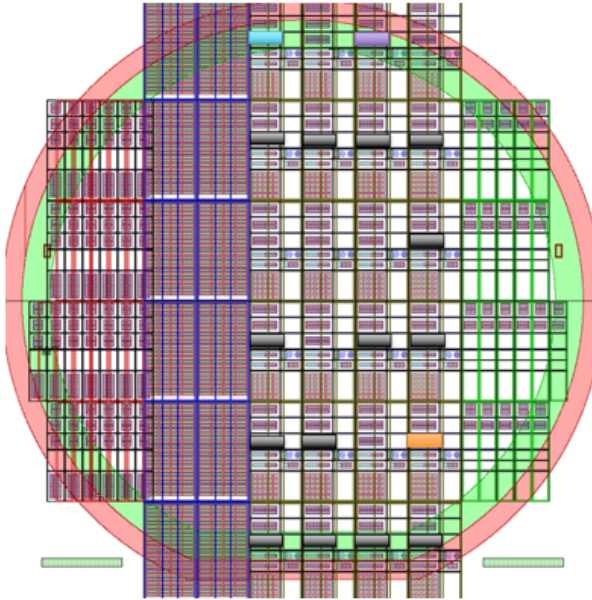


Figure 12. In the upper picture we can identify the gain layer's depletion voltage of the sensors, while in the lower one is shown the sensors' position in the wafer. The colored squares represent the sensors with the lower and the greater voltage depletion. With the black squares, I shown the other measured sensors.

Table 1 summarizes the values of the gain layer depletion voltage. Using these values divided for the gain layer voltage, I calculated the non-uniformity of the wafers. This value is about 2% ($\frac{\Delta V_{GL}}{V_{GL}} * 100$) within a wafer when we exclude sensors at the periphery of the wafers.

Table 1. Wafers from FBK UFSD 3 batch, summary of gain layer depletion.

Wafer	ΔV_{GL}
1	0.46 V
2	0.42 V
3	0.48 V
4	0.42 V

I studied the non-uniformity among different wafers comparing the wafer 3 and 4, as they have similar properties (equal gain layer dose). Omitting the external sensors, which are more doped than the other, I found a difference of 0.54 V in the depletion voltage, that denotes about 2.5% non-uniformity among wafers, as shown in Figure 13.

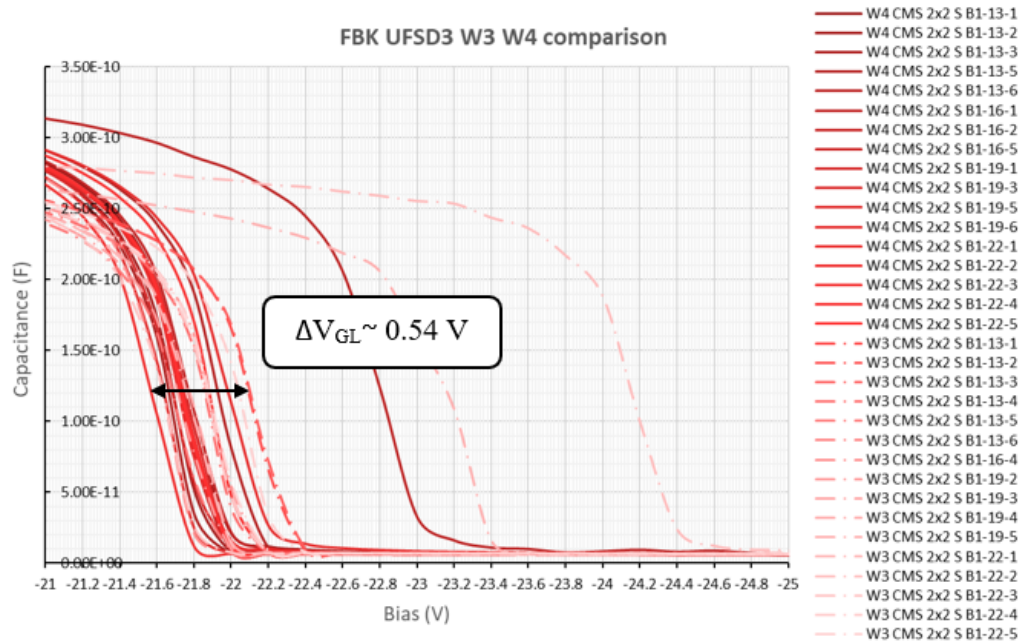


Figure 13. Comparison of wafer 3 and wafer 4 in order to show the uniformity among wafers.

3.1.2 HPK Type 3.2

The second set of devices that I tested are Hamamatsu sensors of geometry. I performed the same measurements I did for the UFSD 3, on 5 different wafers, but this time I analyzed sensors with only a single pad. Also in this case, using $C(V)$ curves for the five wafers analyzed, I studied the gain layer's uniformity, as shown in Figure 14.

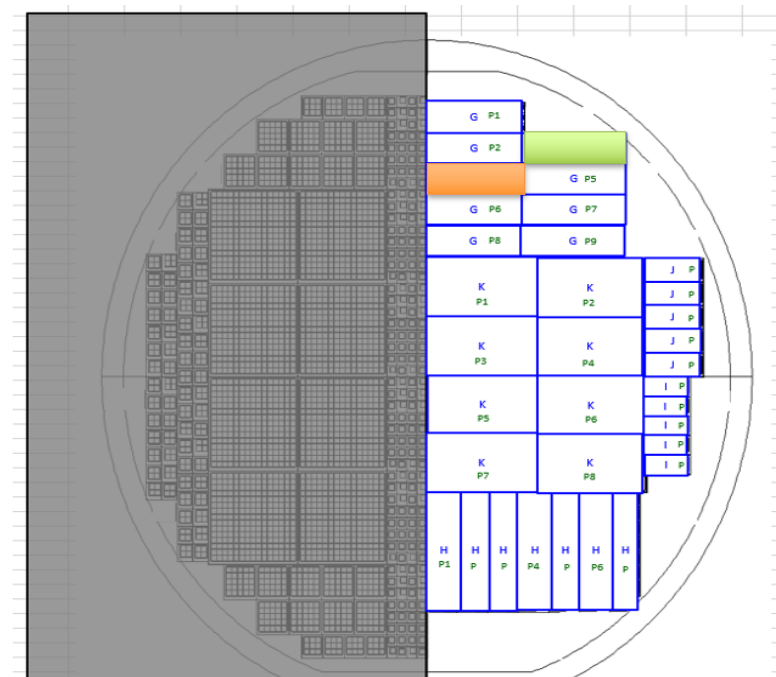
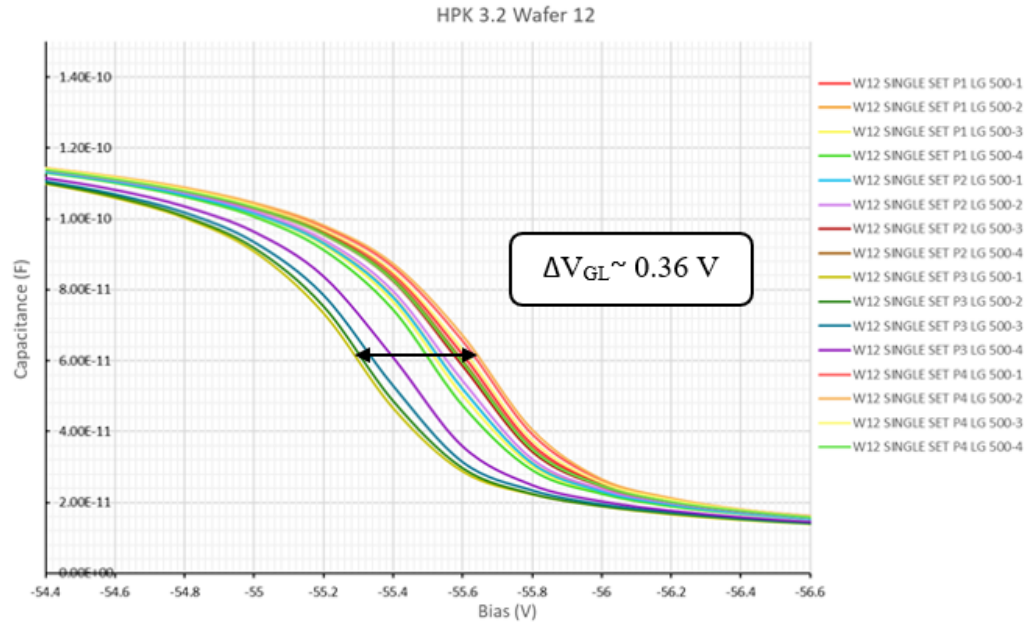


Figure 14. The upper picture shows the depletion voltage of the gain layer for a wafer of HPK type 3.1. The lower one displays the position of the sensors in the wafer. The position in the wafer of the sensor with a large p-gain dose in the gain layer is marked in orange and the detector less doped is marked in green.

Unlike the FBK sensors, the uniformity of the gain layer differs among the measured wafers (Table 2) and they show a non-uniformity between $\sim 0.3\%$ and $\sim 1\%$. I also verified that, in this case, there is not any relation between the position of the sensor in the wafer and the depletion voltage of the sensor.

Table 2. Wafers HPK Type 3.2, summary of gain layer depletion

Wafer	ΔV_{GL}
17	0.16 V
18	0.48 V
11	0.56 V
12	0.36 V
13	0.26 V

Studying wafers that should have equal gain layer dose I was able to measure how large is the non-uniformity of the gain. Figure 15 shows the $C(V)$ curves for sensors coming from five different wafers. For each wafer I selected the two sensors that show the $C(V)$ curves with the smallest and largest depletion voltages. Since the depletion voltage of sensor that depletes earlier and one that depletes later is ~ 0.70 V, the largest non-uniformity across the wafers turned out to be $\sim 1.26\%$.

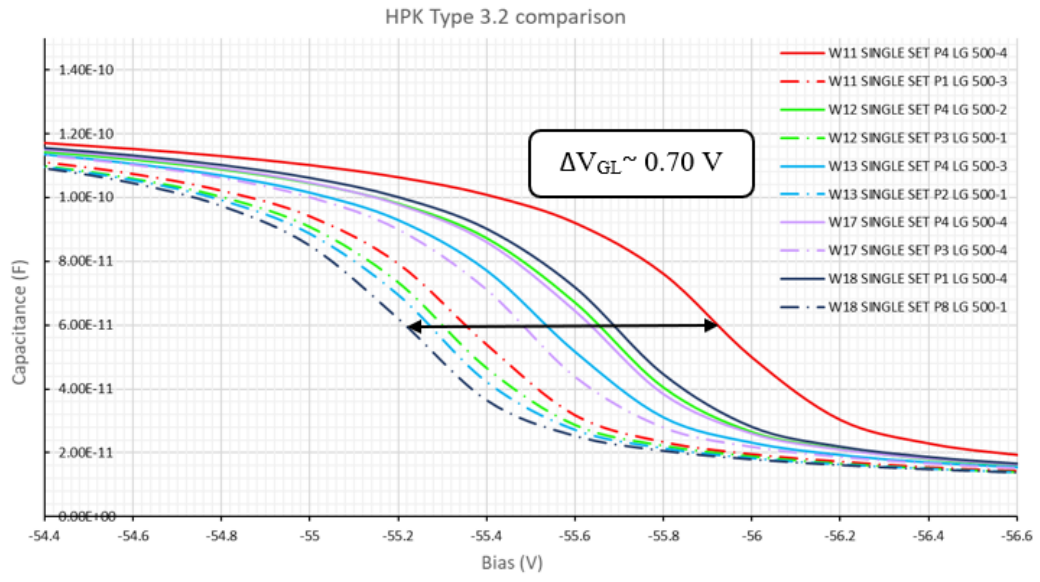


Figure 15. Comparison between C(V) curves for the HPK Type 3.2 (single pad geometry) from five different wafers.

3.1.3 HPK Type 3.1

I also measured the type 3.1 production from Hamamatsu. I studied different geometries, single pad, 2x2 and 4x24 sensors (Figure 16) from different wafers.

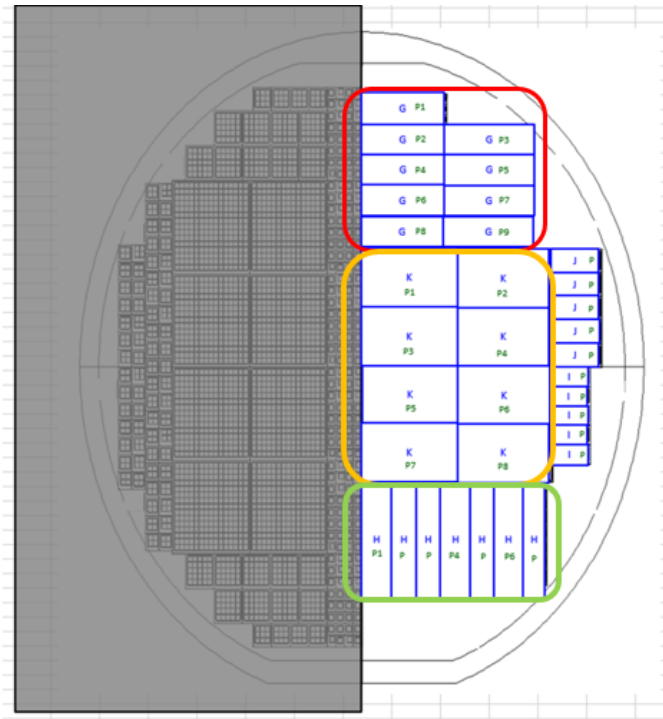


Figure 16. The picture shows the different geometries within an HPK wafer. Red square: single pad sensors; yellow: 4x24 sensors; green: 2x2 sensors.

I measured 16 single pad sensors for each of the five wafers, they show a non-uniformity of the depletion voltage of the gain layer between $\sim 0.5\%$ and $\sim 1\%$. As I did for type 3.2, for each wafer I selected the two C(V) curves that have the largest and smallest depletion voltages, (Figure 17). They have the same nominal implanted dose in the gain layer but it possible to identify a difference of ~ 1.06 V in the depletion voltage among wafers that entails $\sim 2.7\%$ of the non-uniformity of the p-gain dose. As for type 3.2 sensors, this geometry of sensors does not show a relation between the position of the sensors in the wafer and their gain layer doping.

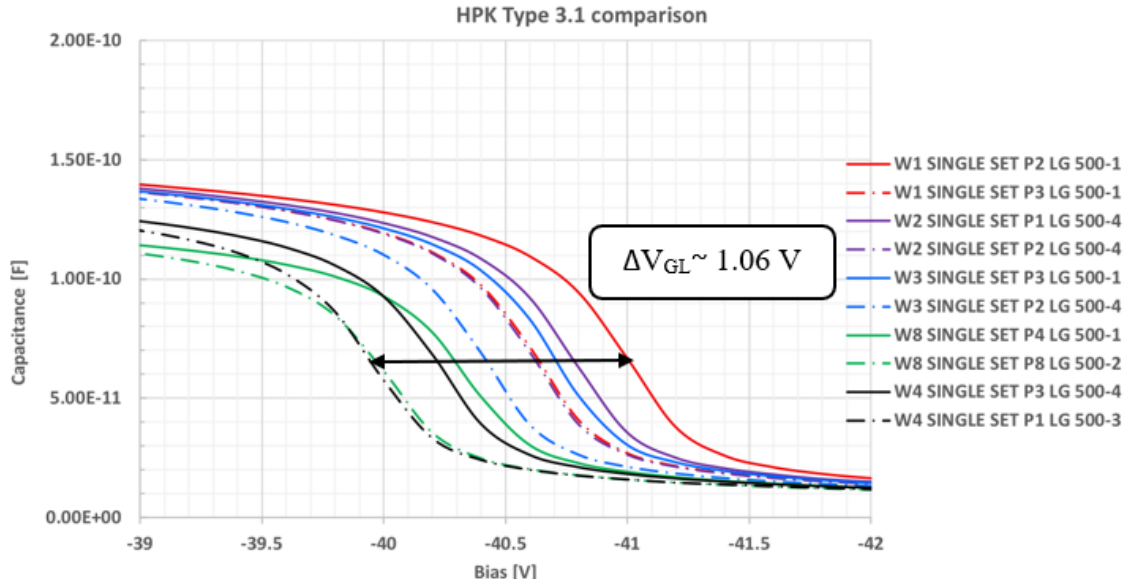


Figure 17. Comparison between $C(V)$ curves for the HPK Type 3.1 from Hamamatsu from five different wafers..

I also studied the 2x2 geometry for wafer 2 and 4. I measured all the four pads of a sensor and about 16 detectors for each wafer. I obtained a non-uniformity of the depletion voltage of $\sim 0.4\%$ and $\sim 0.7\%$ for wafer 2 and 4 respectively. Then I compared them with the respective single pad sensors, as shown in Figure 18, and I found a non-uniformity of the gain of $\sim 1.5\%$ for wafer 2 and $\sim 3.2\%$ for wafer 4. But, as we can see in the Figure 16, the two geometries are positioned on the opposite sides of wafer and with their comparison, it possible to identify a greater doping in the lower part.

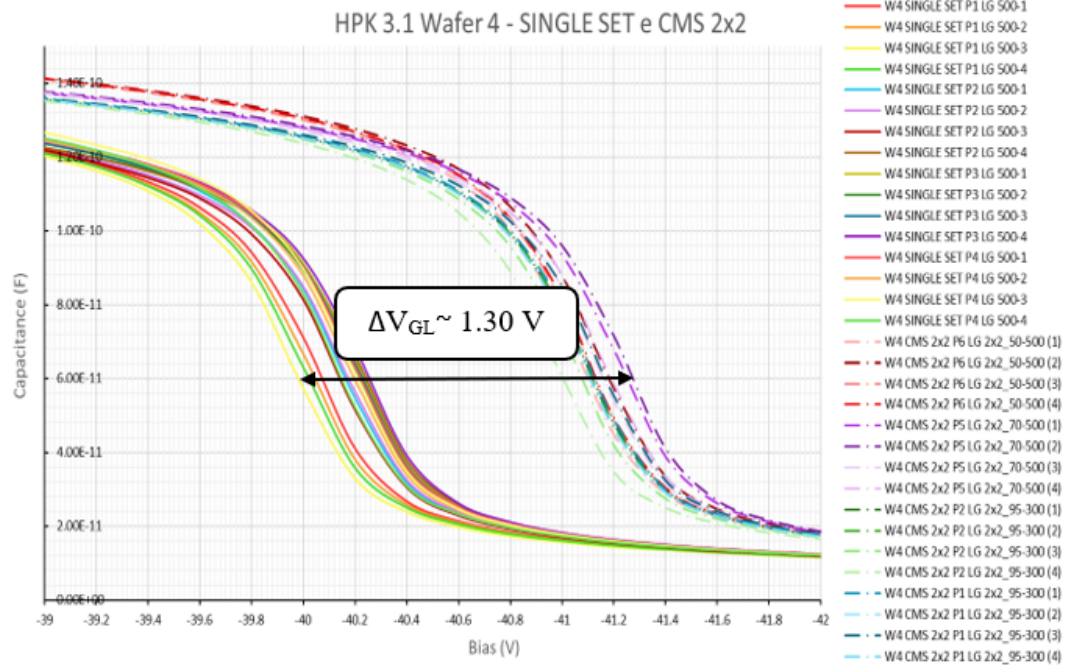


Figure 18. Comparison between single pad and 2x2 sensors (dashed lines) for an HPK wafer.

For the same two wafers, I also measured the 4x24 sensors and for each of them I tested four pads along the detector's diagonal. In this case, I found a non-uniformity of the gain layer of $\sim 2.4\%$ for wafer 2 and $\sim 1.2\%$ for wafer 4. Since the 4x24 geometries are in middle of the wafer (Fig. 16), I expect their depletion curves are enclosed between the single pad and 2x2 detectors. If we observe the Figure 19, it is possible to confirm the expected position of the curves and to identify $\sim 3.2\%$ of the non-uniformity of the p-gain dose.

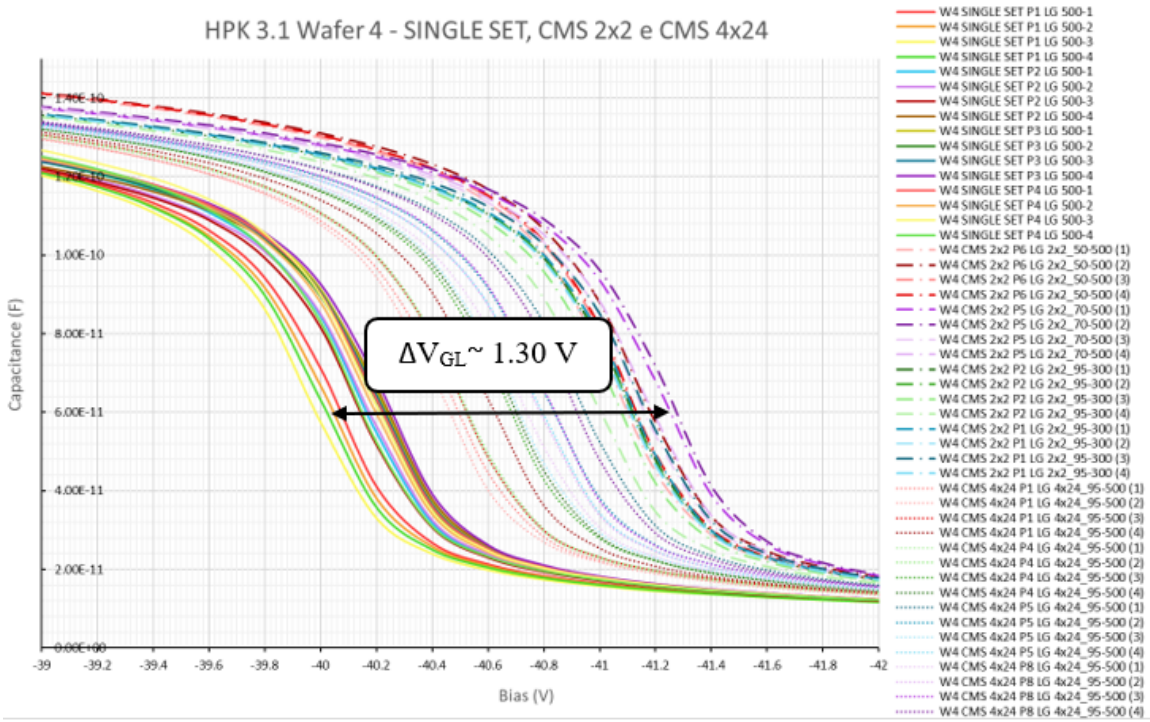


Figure 19. Comparison between single pad (continuous lines), 2x2 (dashed lines) and 4x24 (punctiform lines) sensors for an HPK wafer.

These measurements refer to wafer 4 but I performed the same study for the wafer 2. In both cases it was possible to verify a greater doping of the gain layer in the lower part of the wafer. If we compare the three geometries of wafer 2, we found a non-uniformity of the gain layer of $\sim 2.5\%$. To finish the study on HPK type 3.1, I compared the two C(V) curves with the two most extreme depletion voltages for all the geometry and all the wafers. As shown in Figure 20, I found $\sim 3.7\%$ of the non-uniformity in the whole type 3.1 production.

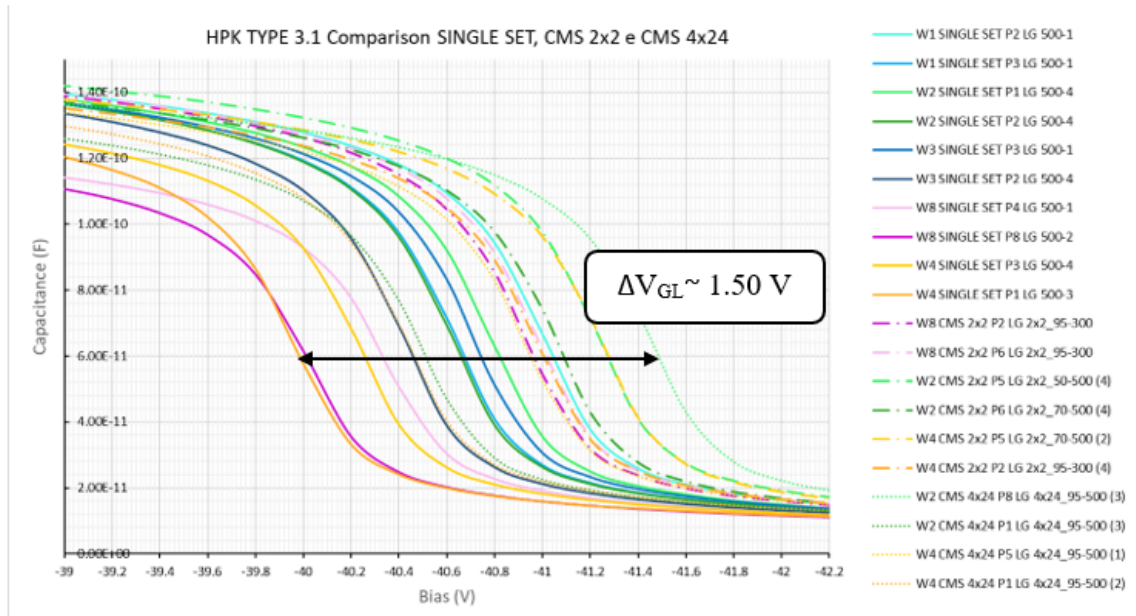


Figure 20. Comparison of all the geometries and all wafers of HPK type 3.1

3.2 Curves from Transient Current Technique

The Transient Current Technique (TCT) is a technique that allows to confirm the gain layer uniformity found through the $C(V)$ curves. I analyzed the wafers of HPK type 3.1 and type 3.2. This method is based on the fact that a more doped gain layers leads to larger signals: comparing the signal from the sensors with the smallest or largest gain layers we should find large signal differences.

3.2.1 HPK Type 3.1

Looking at the Figure 17, I chose to measure two sensors from wafer 1 and 8, one with a large gain layer (W1 max and W8 max) and the other with a small gain layer (W1 min and W8 min), as shown in Figure 21. Two detectors from each wafer are glued on a board (Figure 22) and they are exposed to a laser beam that simulate the passage of a few MIP.

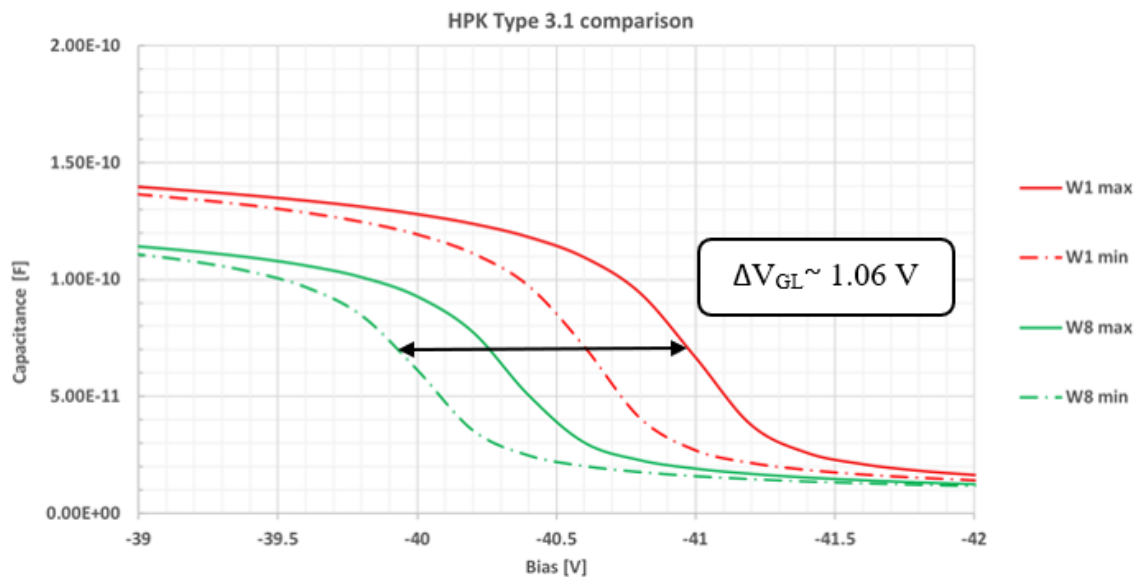


Figure 21. C(V) curves for HPK type 3.1 sensors.

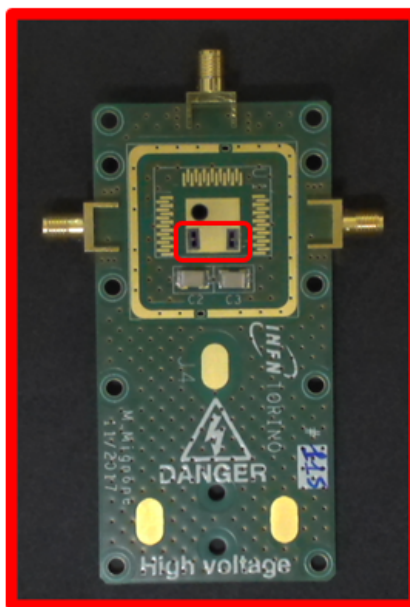


Figure 22. The board used for the TCT measurements. It is possible to observe two glued sensors (red square).

In the test, I provided different bias voltage to the sensor and I recorded the respective values of the signal area on the oscilloscope. To obtain the value of the collected charge from the area value, it is necessary divide it for 50Ω , the input resistance of the oscilloscope: since the area is the product of a (time)*(voltage), dividing it by a resistance I obtain a charge. I measured the collected charge as a function of the applied bias, and I obtained the results displayed in Figure 23. We can

observe that above 150 V (a typical working point of the sensor) to collect the same charge there is ~ 30 V of difference between two sensors with different doping. This is a confirmation of the non-perfect uniformity of the gain layer.

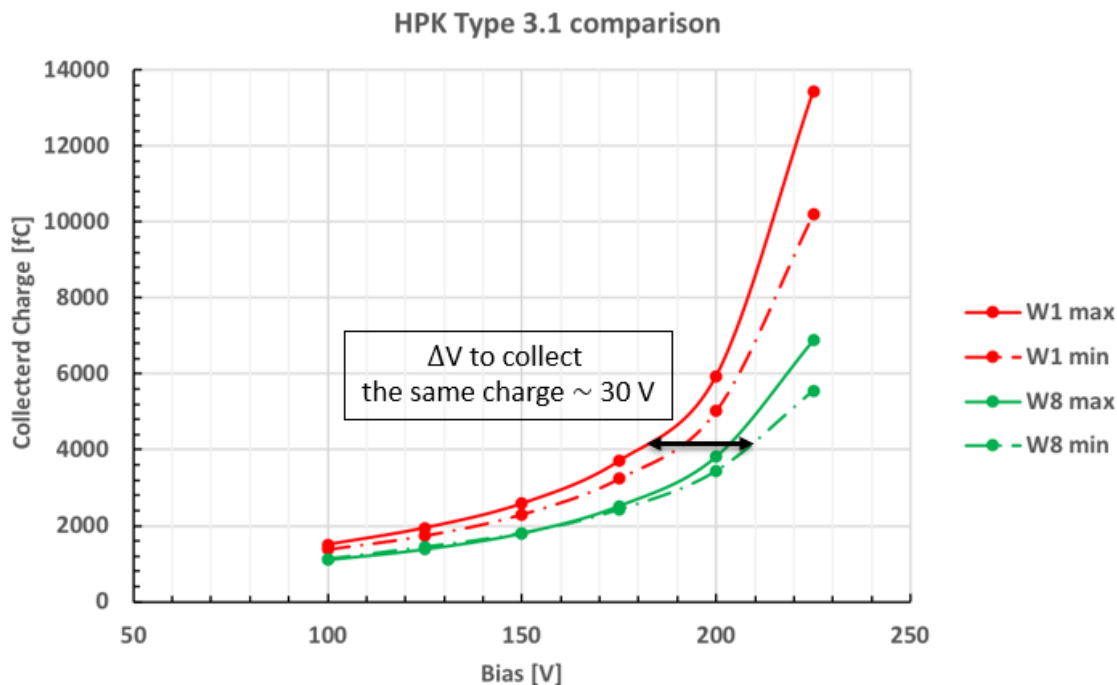


Figure 23. Curves of the collected charge in function of the applied bias for HPK type 3.1

3.2.2 HPK Type 3.2

As I did for HPK Type 3.1, I chose from the $C(V)$ relations displayed in Figure 15 the sensors of wafer 11 and 18 that have a large difference in the gain layer doping and I glued them on a board. As in the previous case, I measured the collected charge as a function of the applied bias and I obtained the graph in Figure 24. This time I performed the measures at a lower bias, because the sensors type 3.2 have a smaller breakdown voltage (this means that, when a high field is applied to the p-n junction, the junction breaks down and there is a very large current). There is about ~ 15 V of difference between two extreme sensors in the $C(V)$ curves to collect the same charge due to the gain layer's non-uniformity.

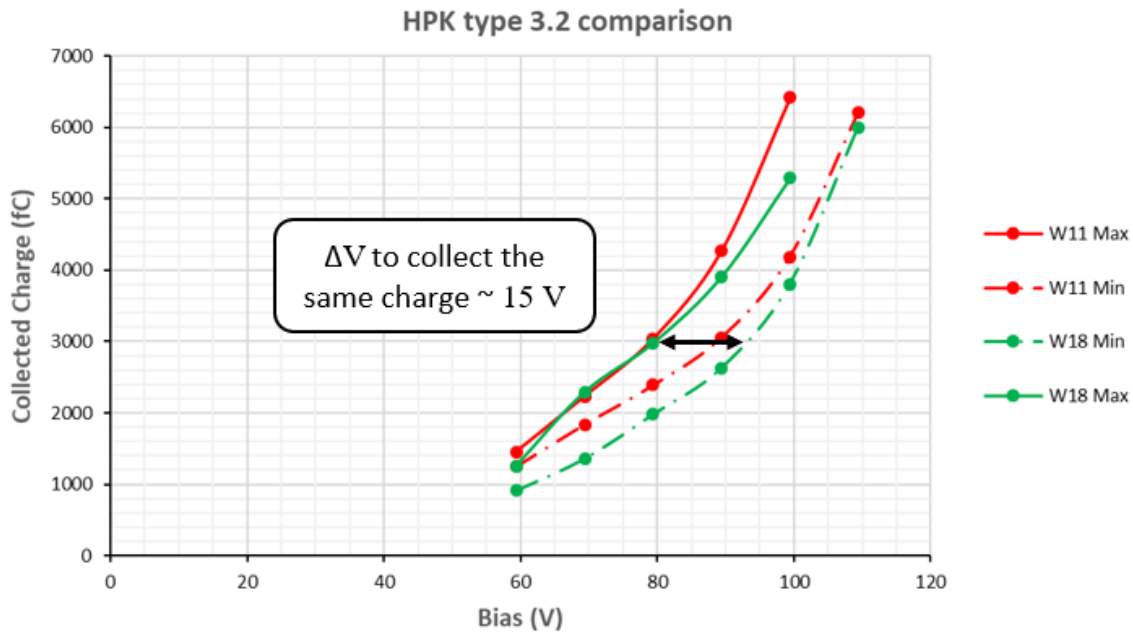


Figure 24. Curves of the collected charge in function of the applied bias for HPK type 3.2

Both for type 3.1 and type 3.2, the relation between the doping of the gain layer and the collected charge is confirmed. If we set a voltage value, we see that the most doped sensor can collect a greater charge than the less doped one.

Conclusions

This thesis is focused on the development and characterization of Low Gain Avalanche Detectors (LGAD), which represent an evolution of silicon detectors with internal charge multiplication. The LGAD technology is at the basis of the development of Ultra-Fast Silicon Detectors (UFSD), thin sensors that use a gain layer in order to achieve charge multiplication and to amplify the signal produced by the passage of a charged particle. In this way, UFSD can provide an excellent space and time measurements.

During my internship at the Laboratory for Innovative Silicon Sensor of the INFN and the department of Physics in Torino, I studied the properties of these detectors and, especially, I probed the uniformity of the internal gain among several sensors. To measure the doping of the gain layer I analyzed the measurements of the $C(V)$ curves, using the probe station set-up, and the curves from the Transient Current Technique (TCT) set up. Through the $C(V)$ curves I could measure a non-uniformity of the gain layer within all the tested wafers and among different wafers. In particular, for Fondazione Bruno Kessler (FBK) production and Hamamatsu Photonics K.K. (HPK) detectors (Type 3.1), I could identify a relation between the position of the sensor in the wafer and the depletion voltage of the sensor. Using the other set-up, the TCT, I measured the sensors response when they are exposed to a laser beam. In this way, I confirmed the non-uniformity of the gain layer and I showed that detectors more doped collect a greater charge than the less doped ones.

Bibliography

- [1] G. Pellegrini et al. “Technology developments and first measurements of Low Gain Avalanche Detectors (LGAD) for high energy physics applications”. In: Nuclear Instruments and Methods in Physics Research A 765 (2014).
- [2] H. Sadrozinski, A. Seiden, N. Cartiglia, “4-Dimensional tracking with Ultra-Fast Silicon Detectors” 2018, Rep. Prog. Phys (81) 026101
- [3] F. Cenna et al. “Weightfield2: A fast simulator for silicon and diamond solid state detector”. In: Nuclear Instruments and Methods in Physics Research A (2015).
- [4] N. Cartiglia et al. “Design optimization of ultra-fast silicon detectors”. In: Nuclear Instruments and Methods in Physics Research A (2015).
- [5] M. Ferrero et al. “Recent studies and characterization of UFSD sensors”. 34th RD50 Workshop - Lancaster, UK, June 12-14 2019.
- [6] A. Picerno. Caratterizzazione di rivelatori al silicio innovativi, Master Thesis. 2014.
- [7] M. Tornago. Development of Ultra-Fast Silicon Detectors for 4D tracking at High Luminosity LHC: laboratory measurements and numerical simulations, Master Thesis. 2019.

Ringraziamenti

Vorrei inizialmente ringraziare Nicolò, Marco, Valentina e Federico per avermi accolta tra loro ed avermi sostenuto in questo periodo di tesi. Grazie a Francesca, e grazie a Flavio, che ha dovuto sopportarmi durante i miei scleri e che continua a farlo.

Un enorme grazie al Prof. Bellan, che se sono arrivata fin qui, in fondo, è anche grazie a lui. Grazie per avermi fatto scoprire questo “bizarro” ma fantastico mondo della fisica e per avermi supportata e sopportata fino a questo momento. Non smetterò mai di ringraziarla per ogni cosa che ha fatto per me.

Grazie a tutti i parenti e amici.

Grazie a Marco, che ha sempre creduto in me e che mi è stato accanto in momenti difficili.

E infine, grazie ai miei genitori per la loro pazienza e perchè mi stanno permettendo di raggiungere un sogno.